

Phase diagram of $Z(N)$ and $U(1)$ gauge theories in three dimensions

Gyan Bhanot and Michael Creutz

Physics Department, Brookhaven National Laboratory, Upton, New York 11973

(Received 5 February 1980)

We present Monte Carlo studies of $Z(N)$ and $U(1)$ lattice gauge theories in three space-time dimensions. The $Z(N)$ gauge theory is analyzed via its dual spin system. We find that $Z(N)$ has one phase transition that moves to zero temperature as $N \rightarrow \infty$. The $U(1)$ theory has only a single, confining phase. A study of Wilson loops in $Z(8)$ shows that the coefficient of the area law vanishes for all temperatures below the critical temperature. No such zero is seen in the string tension for $U(1)$ gauge theory. We also study the $U(1)$ gauge theory in five dimensions and see a clear signal for a first-order phase transition.

I. INTRODUCTION

Lattice gauge theory was introduced by Wilson¹ as a method of understanding quark confinement. The lattice formulation of field theory preserves local gauge invariance as an exact symmetry on the lattice and the lattice spacing provides an ultraviolet cutoff, rendering the theory finite. One feature of the lattice theory is that in strong coupling the theory confines charge. If it can be shown that quantum chromodynamics (QCD) has only a single phase, the lattice theory explains the absence of quarks and gluons in final states of hadronic interactions.

However, this same property of confinement proves to be an embarrassment for the lattice version of QED, for we know that QED must be able to describe unconfined electrons and photons. The theory must find a way out of this dilemma by undergoing a phase transition at finite coupling, separating a strongly coupled, confining phase from a weakly coupled phase without confinement. It is known² that if the dimensionality of space is high enough, a phase transition always occurs for any lattice gauge theory. Recent Monte Carlo studies³ have shown that the lattice $U(1)$ theory in four dimensions has two phases. It is believed^{4,5} that $d=4$ is a critical dimension for the lattice $U(1)$ theory. For $D < 4$ the theory exists only in a confining phase, whereas for $d \geq 4$ there are at least two phases.

Rather strong theoretical arguments indicate the absence of phase transitions in three-dimensional $U(1)$ lattice gauge theory. Polyakov has suggested that the excitation of extended topologically nontrivial configurations will preclude the occurrence of an ordered low-temperature phase.⁵ Drell, Quinn, Svetitsky, and Weinstein have rephrased this argument in a Hamiltonian variational formalism.⁶ Thus, this model represents a simple but nontrivial example of confinement for all values of coupling, analogous to the expected behavior of non-Abelian gauge theory in four dimen-

sions.

We have performed a Monte Carlo study of the $U(1)$ lattice gauge theory in three Euclidean dimensions both directly as well as via the limit $N \rightarrow \infty$ of a $Z(N)$ lattice gauge theory. The $Z(N)$ theory was studied by analyzing its dual—which is a $Z(N)$ spin theory. We use the hysteresis cycle of Ref. 3 as our signal of the phase transition.

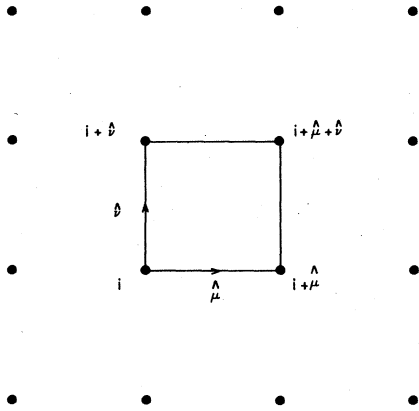
Hysteresis cycles of $Z(N)$ theory for $N=2, 3, 4, 5, 6, 8, 10, 12$, and 20 show clear evidence for a phase transition at a temperature $T_c(N)$ which vanishes as $N \rightarrow \infty$ roughly as $1/N^2$.⁷ A similar hysteresis cycle of $U(1)$ gauge theory shows no evidence for a phase transition. Finally, a hysteresis cycle of $U(1)$ gauge theory in five dimensions unearths a well-defined first-order phase transition.

We have also studied Wilson loops in $Z(8)$ and $U(1)$ gauge theory. We calculate the coefficient of the area law¹ as a function of the inverse temperature β . For $Z(8)$, we find that this coefficient is consistent with zero for β greater than the critical temperature of the $Z(8)$ theory. In the $U(1)$ theory, the coefficient of the area law is the string tension times the lattice spacing squared.⁸ Our results suggest that the $U(1)$ string tension does not become zero for any finite β . This analysis is evidence that the $U(1)$ theory in three dimensions has only a single phase.

This paper is organized as follows: In Sec. II, we define the $Z(N)$ and $U(1)$ theories. Section III provides an explanation of the Monte Carlo procedure and the hysteresis cycle. Section IV A reviews known results from $Z(N)$ duality for $N \leq 4$. In Section IV B, we enumerate the duality results we use in our analysis. Section V is a discussion of our results and Sec. VI contains a brief summary.

II. THE MODELS

$Z(N)$ lattice gauge theory is defined in terms of the elements $U_{i,\mu}$ of the gauge group. These

FIG. 1. The plaquette $(i, \hat{\mu}, \hat{\nu})$.

U 's live on the links of a hypercubical lattice. The set of all possible U 's on a link is an Abelian group under multiplication. The U 's are parametrized by an integer $n \pmod{N}$ according to

$$U_{j, \hat{\mu}} = \exp\left(i \frac{2\pi}{N} n_{j, \hat{\mu}}\right), \quad n_{j, \hat{\mu}} = 0, 1, 2, \dots, N-1. \quad (2.1)$$

The index j labels the sites of the lattice and $\hat{\mu} = 1, 2, \dots, d$ is the unit vector in the μ direction. The action is chosen to be invariant under $Z(N)$ transformations and as local as possible. It is given by

$$S_N(\{U\}) = \sum_{(i, \hat{\mu}, \hat{\nu})} [1 - \text{Re}(U_{i, \hat{\mu}} U_{i+\hat{\nu}, \hat{\nu}} U_{i+\hat{\nu}, \hat{\mu}}^* U_{i, \hat{\nu}}^*)]. \quad (2.2)$$

The set $(i, \hat{\mu}, \hat{\nu})$ defines a plaquette in the lattice as shown in Fig. 1. The sum in (2.2) is over all plaquettes in the lattice, each plaquette being counted only once, and U^* is the complex conjugate of U . To minimize boundary effects, we enforce periodic boundary conditions.

A more convenient way of writing the action is

$$S_N(\{n\}) = \sum_{(i, \hat{\mu}, \hat{\nu})} \left[1 - \cos\left(\frac{2\pi}{N} n_{\hat{\mu}\hat{\nu}}(i)\right)\right] \quad (2.3)$$

with

$$n_{\hat{\mu}\hat{\nu}}(i) = n_{i, \hat{\mu}} + n_{i+\hat{\nu}, \hat{\nu}} - n_{i+\hat{\nu}, \hat{\mu}} - n_{i, \hat{\nu}}. \quad (2.4)$$

The partition function Z_N is a sum over the Boltzmann weights of the lattice configurations $\{n\}$,

$$Z_N(\beta) = \sum_{\{n\}} \exp[-\beta S_N(\{n\})]. \quad (2.5)$$

In (2.5), β is the inverse temperature.

The $U(1)$ theory is defined as the $N \rightarrow \infty$ limit of

(2.1), (2.3), and (2.5). The $U_{j, \hat{\mu}}$'s are now parametrized by an angle $\theta_n(j)$,

$$U_{j, \hat{\mu}} = \exp[i\theta_{\hat{\mu}}(j)], \quad \theta_{\hat{\mu}}(j) \in [-\pi, \pi]. \quad (2.6)$$

The action for the $U(1)$ theory is

$$S_{U(1)}(\{\theta\}) = \sum_{(i, \hat{\mu}, \hat{\nu})} [1 - \cos \theta_{\hat{\mu}\hat{\nu}}(i)], \quad (2.7)$$

where

$$\theta_{\hat{\mu}\hat{\nu}}(i) = \theta_{\hat{\mu}}(i) + \theta_{\hat{\nu}}(i + \hat{\mu}) - \theta_{\hat{\mu}}(i + \hat{\nu}) - \theta_{\hat{\nu}}(i). \quad (2.8)$$

$\theta_{\hat{\mu}\hat{\nu}}$ is the lattice version of the curl of the θ field. The partition function for the $U(1)$ theory is

$$Z_{U(1)}(\beta) = \sum_{\{\theta\}} \exp[-\beta S_{U(1)}(\{\theta\})]. \quad (2.9)$$

The free energy per plaquette is given by

$$F(\beta) = \frac{1}{N_p} \ln F(\beta), \quad N_p = \text{number of plaquettes}. \quad (2.10)$$

We define our order parameter $E(\beta)$ as

$$E(\beta) = -\frac{\partial F(\beta)}{\partial \beta} = \begin{cases} \left\langle 1 - \cos\left(\frac{2\pi}{N} n_{\hat{\mu}\hat{\nu}}\right) \right\rangle & \text{for } Z(N), \\ \langle 1 - \cos(\theta_{\hat{\mu}\hat{\nu}}) \rangle & \text{for } U(1). \end{cases} \quad (2.11)$$

An n th-order phase transition is a discontinuity in the $(n-1)$ th derivative of $E(\beta)$.

The β in (2.9) may be interpreted either as the inverse temperature or the inverse coupling constant squared of the corresponding continuum theory. If the theory has a phase transition for finite β , the coupling-constant interpretation applies in the phase which includes the point $\beta = \infty$. To see this, consider the limit of large β . The action (2.7) is minimized by configurations for which the θ field varies slowly over the lattice. For such configurations, $\theta_{\hat{\mu}\hat{\nu}}$ is small compared to 2π and the cosine in (2.7) may be expanded to lowest nontrivial order. This gives the partition function $\bar{Z}(\beta)$ of the $U(1)$ theory in the spin-wave approximation,

$$\bar{Z}(\beta) = \lim_{\beta \rightarrow \infty} Z_{U(1)}(\beta) = \sum_{\{\theta\}} \exp\left[-\frac{\beta}{2} \sum_{(i, \hat{\mu}, \hat{\nu})} \theta_{\hat{\mu}\hat{\nu}}^2(i)\right]. \quad (2.12)$$

To define the continuum limit, we introduce the gauge field $A_{\hat{\mu}}(i)$ through

$$A_{\hat{\mu}}(i) = \frac{1}{a} \theta_{\hat{\mu}}(i). \quad (2.13)$$

Since the range of θ is $(-\pi, \pi)$, the range of the A field is $(-\pi/a, \pi/a)$. In the continuum limit $a \rightarrow 0$, the range of A is unbounded. It is clear that $1/a$ also acts as a momentum-space cutoff. The field A on the lattice has Fourier components up to $1/a$ but not higher. The lattice may be viewed as a mechanism to introduce a gauge-invariant momentum-space cutoff in the theory.¹

In terms of the A field, the partition function becomes

$$\bar{Z}(\beta) = \left[\prod_{(x, \mu)} \int_{-\pi/a}^{+\pi/a} dA_\mu(x) \right] \times \exp \left(-\frac{\beta a^{4-d}}{2} \int d^4x \sum_{\mu > \nu} F_{\mu\nu} F_{\mu\nu} \right) \quad (2.14)$$

with

$$F_{\mu\nu} = \partial_\mu A_\nu - \partial_\nu A_\mu. \quad (2.15)$$

(2.14) is immediately identified as the usual "sum over histories" for the U(1) theory if we identify the U(1) coupling constant e^2 as

$$e^2 = (\beta a^{4-d})^{-1}. \quad (2.16)$$

There is an interesting inference that can be drawn from (2.16). The theory described by (2.14) is one of free, massless photons. The analogy (2.16) states that for $d < 4$, the spin-wave approximation (2.12) survives the continuum limit ($a \rightarrow 0$) only for $\beta = \infty$. This suggests that the spin-wave phase is absent in the continuum limit of U(1) lattice gauge theories for $d \leq 3$. This argument is merely suggestive and should not be construed as proof. It is important to note that the same argument cannot rule out a spin-wave phase for $d = 4$.

III. THE MONTE CARLO TECHNIQUE

A. Algorithm for the partition function

The idea is to generate configurations of fields on a finite lattice in such a way that the ensemble of such configurations simulates the partition function. Once these configurations are at hand, it is a simple matter to find the ensemble average of any function of the field variables.

The procedure we use to bring the lattice to statistical equilibrium at any given β is the heat-bath method of Creutz, Jacobs, and Rebbi.³ This will now be briefly discussed.

The lattice must first be set in an initial configuration. One possible initial configuration is to set all the variables to the identity element of the gauge group. This ordered configuration corresponds to zero temperature or infinite β . Alternately, the initial lattice variables are picked randomly from the gauge group. This disordered configuration corresponds to infinite temperature

or zero β .

Once the lattice has been set in an initial configuration, we sequentially change each variable to a new value chosen from the gauge group in the following manner: Let x denote the variable being processed. Define the function

$$f(x) = \exp[-\beta \mathcal{S}(x, \{\phi\})], \quad (3.1)$$

where $\{\phi\}$ is the set of variables which directly interact with x , and $\mathcal{S}(x, \{\phi\})$ is the action from this interaction. The function $f(x)$ defines a probability distribution for x . We replace the variable being processed by another distributed as $f(x)$. This procedure is repeated for each variable in the lattice. While one variable is being changed, all others are kept fixed. One such sweep of the lattice is called an iteration. The lattice approaches thermal equilibrium at a given β when several iterations are performed at that β . This procedure has been shown to give rapid convergence to statistical equilibrium in regions far from phase transitions.^{3,8}

B. Hysteresis cycle

Starting from an ordered configuration and a large value β_0 for β , the lattice is heated to $\beta=0$ in discrete steps and then recooled to β_0 . A number of iterations are performed at fixed β until the value of $E(\beta)$ has stabilized. We go to the next value of β in the cycle when the average value of $E(\beta)$ over two sets of three iterations does not differ by more than a prescribed tolerance. If the theory has a phase transition at some β between 0 and β_0 , a hysteresis effect is seen in $E(\beta)$. This effect is much like the hysteresis in the magnetization as a function of applied field which is observed in ferromagnets near the Curie point. It is caused by the slow convergence of the Monte Carlo procedure because the relaxation time of the near critical system is large compared to the unit of time that corresponds to one iteration of the lattice (or, alternately, when the relaxation time is large compared to the average time scale of the interaction).

IV. DUALITY AND Z(N) GAUGE THEORY

A. $N \leq 4$

Geometrical duality⁹ in d dimensions associates q -dimensional manifolds with $(d-q)$ -dimensional manifolds. In three dimensions duality associates links to plaquettes and sites to cubes. Thus, the dual of the gauge theory, where the action is defined on plaquettes, is a spin theory with the action defined on links. The local invariance of the gauge theory is reduced to a global invariance in the spin system.

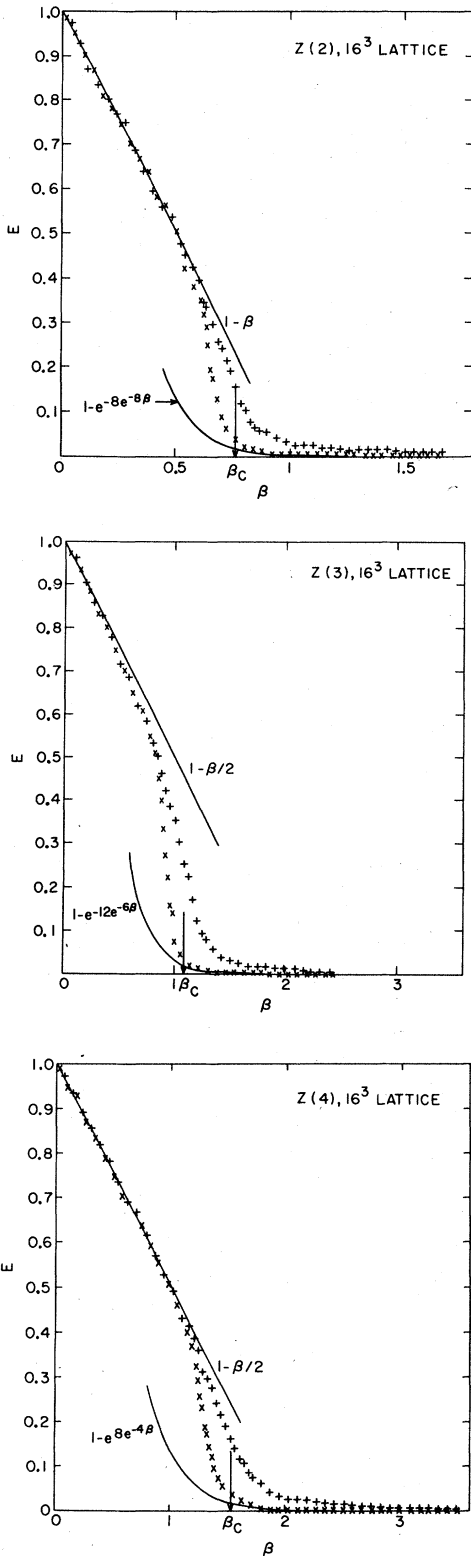


FIG. 2. Hysteresis cycles of three-dimensional $Z(2)$, $Z(3)$, and $Z(4)$ gauge theory on a 16^3 lattice. Five iterations were performed at each β before measuring $E(\beta)$.

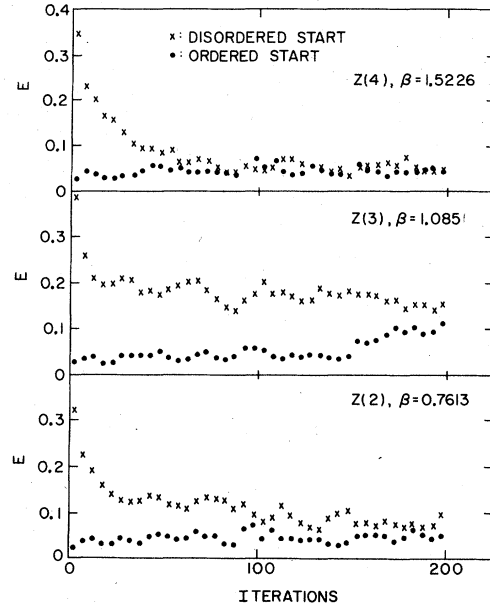


FIG. 3. Iterations at the critical point for ordered and random initial conditions in three-dimensional $Z(2)$, $Z(3)$, and $Z(4)$ gauge theory.

Duality in $Z(N)$ theory has been the subject of numerous investigations in recent years.¹⁰⁻¹² The critical behavior of $Z(N)$ gauge theory in three dimensions for $N \leq 4$ follows from the known critical behavior of its dual spin system. We now summarize these results:

For $N \leq 4$, the $Z(N)$ gauge theory is dual to a spin theory with action defined by

$$S_{N, \text{spin}}(\{s\}) = \frac{kN}{2} \sum_{\langle ij \rangle} (s_i s_j^{-1} + \text{c.c.}), \quad (4.1)$$

where the sum is over nearest neighbors and s_i is an element of $Z(N)$ on the sites of a hypercubical lattice.

The duality relations relate the coupling k of the spin theory to β , the gauge coupling.¹⁰ Thus,

$$e^{-2\beta} = \tanh k \quad \text{for } Z(2), \quad (4.2a)$$

$$e^{-3\beta/2} = \frac{1 - e^{-3k/2}}{1 + 2e^{-3k/2}} \quad \text{for } Z(3), \quad (4.2b)$$

$$e^{-\beta} = \tanh k/2 \quad \text{for } Z(4). \quad (4.2c)$$

The critical points of the $Z(N)$ spin theory for $N \leq 4$ are known. For $N=2$, the spin theory is an Ising model known to have a transition in three dimensions at $k_{2c} = 0.22171$.¹³ The $Z(3)$ spin theory, or equivalently, the three-state Potts model, has a first-order transition at $k_{3c} = 0.367$.¹⁴ Finally, the partition function of the $Z(4)$ spin theory in three dimensions factorizes into a product of two independent $Z(2)$ spin systems, each with

half the coupling strength.¹⁵ This gives $k_{4c} = 2k_{2c} = 0.44342$.

Using (3.2), this gives the critical points for $Z(2)$, $Z(3)$, and $Z(4)$ gauge theories:

$$\begin{aligned} \beta_{2c} &= 0.7613 \text{ (Ref. 16)}, & \beta_{3c} &= 1.085, \\ \beta_{4c} &= 2\beta_{2c} = 1.5226. \end{aligned} \quad (4.3)$$

We present Monte Carlo results for $N=2, 3$, and 4 in Figs. 2 and 3. Figures 2(a)–2(c) are hysteresis cycles for the $Z(2)$, $Z(3)$, and $Z(4)$ gauge theories and the hysteresis effects in the regions of the critical points of (4.3) are clearly visible. Figure 3 shows plots of $E(\beta)$ versus iterations at the critical points in these theories starting from ordered and disordered lattices. The plotted points are the average value of $E(\beta)$ over five iterations. The rapid convergence of $E(\beta)$ to an equilibrium value for $Z(2)$ and $Z(4)$ indicates a continuous transition. The $Z(3)$ data show a much slower convergence in agreement with other experiments which have shown this transition to be a rather peculiar kind of first-order transition.¹⁴

B. Arbitrary N

The reason why a $Z(N)$ spin theory is preferable to working directly on the $Z(N)$ gauge theory is the following. We shall see that as N increases, the critical point of the $Z(N)$ theory moves out to large β roughly as N^2 . For very large β , the lattice is highly ordered (very cold) and the hysteresis effect that we use as a signal of the transition is very weak. In particular, on the cooling cycle, the lattice converges very slowly to equilibrium beyond the critical point and the hysteresis loop tends not to close for high β . As a consequence, the critical region is not well defined. The duality transformation, roughly speaking, maps low temperatures into high temperatures and vice versa. Thus, the highly ordered, slowly converging configurations of the gauge theory near its critical point are mapped into highly disordered, high-temperature configurations of the spin theory by the duality transformation. It is then very easy to get a good hysteresis signal for the transition because the hot dual lattice converges rapidly to equilibrium on both sides of the critical point.

We now review duality in $Z(N)$ gauge theory.¹² The partition function is

$$Z_N(\beta) = \sum_{\{n\}} \prod_{(i, \hat{\mu}, \hat{\nu})} \exp \left[\beta \cos \left(\frac{2\pi}{N} n_{\mu\nu}(i) \right) \right] \quad (4.4)$$

with $n_{\mu\nu}$ defined by (2.4).

We perform a finite Fourier transform on Z_N .

Thus,

$$\begin{aligned} \exp \left[\beta \cos \left(\frac{2\pi}{N} n_{\mu\nu}(i) \right) \right] \\ = \sum_{l_{\mu\nu}=0}^{N-1} I_{l_{\mu\nu}}(\beta) \exp(2\pi i n_{\mu\nu} l_{\mu\nu} / N). \end{aligned} \quad (4.5)$$

The inverse transformation is

$$\begin{aligned} I_{l_{\mu\nu}}(\beta) &= \frac{1}{N} \sum_{n_{\mu\nu}=0}^{N-1} \exp \left[\beta \cos \left(\frac{2\pi}{N} n_{\mu\nu} \right) \right] \\ &\quad \times \exp(-2\pi i n_{\mu\nu} l_{\mu\nu} / N) \end{aligned} \quad (4.6)$$

and the partition function becomes

$$Z_N(\beta) = \sum_{\{n\}} \sum_{\{l\}} \prod_{(i, \hat{\mu}, \hat{\nu})} I_{l_{\mu\nu}}^{(i)}(\beta) \exp[2\pi i l_{\mu\nu}(i) n_{\mu\nu}(i) / N]. \quad (4.7)$$

At this stage, we introduce the dual lattice. It is defined as a set of points shifted from the points of the original lattice by half a lattice spacing in every direction. With each plaquette of the original lattice we associate the link of the dual lattice that intersects it. We further imagine the l variables in (4.7) to live on the links of the dual lattice. Now perform the sum in (4.7) over the link variables $\{n\}$. The result is

$$Z_N(\beta) = \sum_{\{l\}} \prod_{(i, \hat{\mu}, \hat{\nu})} I_{l_{\mu\nu}}^{(i)}(\beta) \delta_{[\sum_{\hat{\mu}, \hat{\nu}} * l_{\mu\nu}(i), 0 \pmod{N}]}. \quad (4.8)$$

The constraint on the $l_{\mu\nu}$'s in (4.9) is as follows: Each link of the original lattice is connected to four plaquettes. These plaquettes each have $l_{\mu\nu}$ associated with their dual link. These four $l_{\mu\nu}$'s form a plaquette on the dual lattice. The constraint in (4.8) requires the vanishing of the sum of $l_{\mu\nu}$'s on all plaquettes of the dual lattice. We represent this pictorially in Fig. 4. The dots in the figure represent the sites of the original lattice and the crosses define the dual lattice sites. When we perform the sum in (4.7) over the link

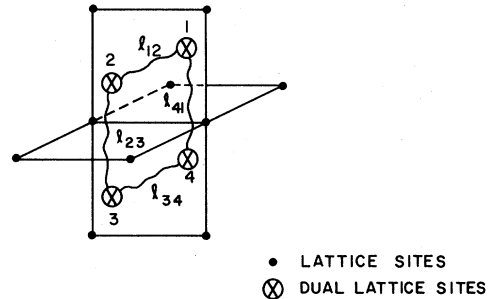


FIG. 4. Showing the constraint of Eq. (4.8) pictorially. The dots are the sites of the lattice and the crosses are sites of the dual lattice.

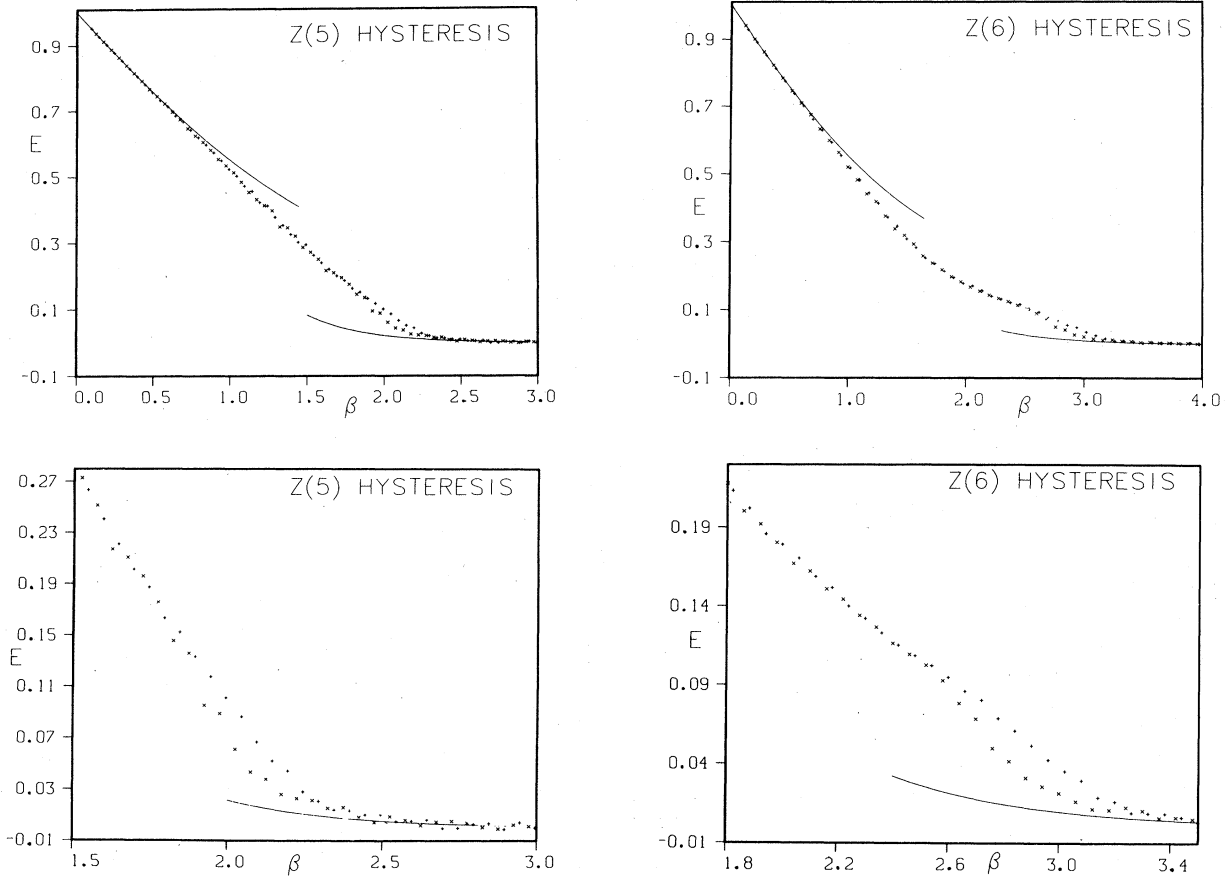


FIG. 5. Hysteresis cycles in three-dimensional $Z(N)$ gauge theory for $N=5, 6, 8, 10, 12, 20$ on a 16^3 lattice.

AB of Fig. 4, we generate the constraint $l_{12} + l_{23} + l_{34} + l_{41} = 0 \pmod{N}$. The solution of the constraint is¹⁵

$$l_{\mu\nu} = \frac{N}{2\pi i} \ln(s_\mu s_\nu^{-1}), \quad (4.9)$$

where s_μ is an element of $Z(N)$ on the sites of the dual lattice. The proof that (4.9) solves the constraint is clear from Fig. 4. We have

$$l_{12} + l_{23} + l_{34} + l_{41} = \frac{N}{2\pi i} \ln(s_1 s_2^{-1} s_2 s_3^{-1} s_3 s_4^{-1} s_4 s_1^{-1}) = 0. \quad (4.10)$$

The partition function is now a sum over configurations on the dual lattice

$$Z_N(\beta) = \sum_{\{s\}} \exp\left(\sum_{\langle\mu\nu\rangle} \ln I_{l_{\mu\nu}}(\beta)\right), \quad (4.11)$$

where the sum is over all nearest neighbors $\langle\mu\nu\rangle$ on the dual lattice, $l_{\mu\nu}$ is an integer valued field ($l_{\mu\nu} = 0, 1, \dots, N-1$) defined from the $Z(N)$ spins at the sites of the dual lattice by (4.9), and $I_{l_{\mu\nu}}(\beta)$

is defined by (4.6). The action on the dual lattice is therefore

$$S_{\text{dual}, N} = \sum_{\langle\mu\nu\rangle} \ln I_{l_{\mu\nu}}(\beta). \quad (4.12)$$

Notice that the form (4.12) of the action is local and therefore well suited to the Monte Carlo procedure we described in Sec. III A.

Finally, we discuss the Wilson loop operator as a correlation function on the dual lattice. The Wilson loop is defined as the expectation value of the product of U 's around a closed curve C . Thus,

$$\begin{aligned} W_C(\beta) &= \left\langle \prod_C U \right\rangle \\ &= \frac{1}{Z_N(\beta)} \sum_{\{n\}} \left(\prod_C U \right) \exp[-\beta S(\{n\})]. \end{aligned} \quad (4.13)$$

Consider an arbitrary surface bounded by C and made up of r plaquettes p_1, p_2, \dots, p_r . Let $l_{\mu\nu}(m)$, $m = 1, 2, \dots, r$ be the variables on links dual

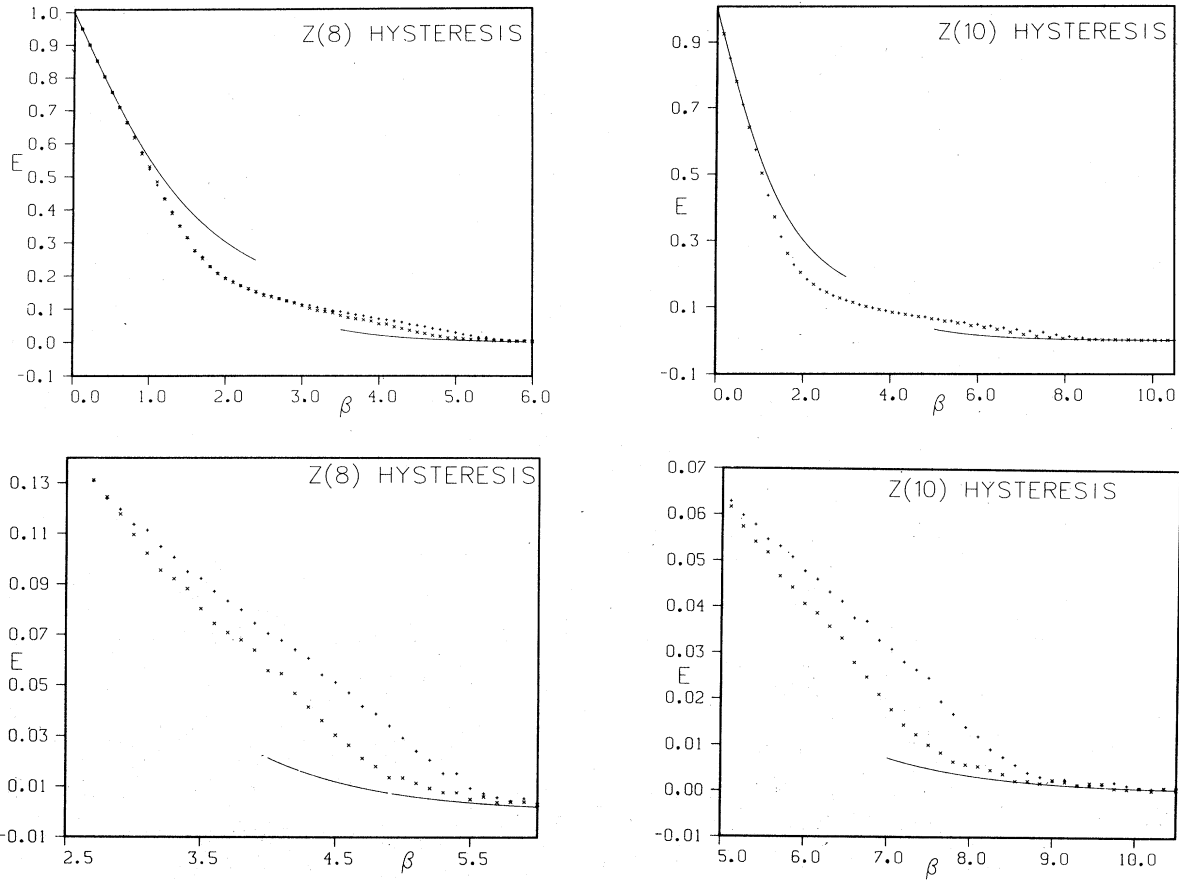


FIG. 5. (Continued).

to these plaquettes. It is shown in Ref. 11 that

$$W_C(\beta) = \left\langle \prod_{m=1}^r \frac{I_{l_{\mu\nu}(m)+1}(\beta)}{I_{l_{\mu\nu}(m)}(\beta)} \right\rangle, \quad (4.14)$$

where the expectation value is evaluated in the dual lattice using the partition function (4.11).

In particular, when C is the boundary of a single plaquette, we get

$$W_1(\beta) = 1 - E(\beta) = \langle I_{l_{\mu\nu}+1}(\beta) / I_{l_{\mu\nu}}(\beta) \rangle. \quad (4.15)$$

It is easy to see that (4.15) is physically sensible. For large β , the dual lattice is hot and the $l_{\mu\nu}$'s random. Hence, W_1 is near unity and $E(\beta)$ near zero. Conversely, for small β , the dual lattice is cold and most $l_{\mu\nu}$'s vanish. Hence $W_1 \rightarrow I_1/I_0 \sim \beta/2$ for small β [except for $Z(2)$, where $W_1 \sim \beta$ for small β], which means that $E(\beta)$ is near unity. This is indeed what one expects for $E(\beta)$ and $W_1(\beta)$. In our computer simulations of the $Z(N)$ gauge theory, we use the dual form (4.11) of the partition function and evaluate $W_C(\beta)$ directly from the spin theory using (4.14). For the $U(1)$

theory, however, we work with the gauge theory on the original lattice.

V. RESULTS

In Figs. 5(a)–5(f), we present hysteresis cycles of $E(\beta)$ for $Z(5)$, $Z(6)$, $Z(8)$, $Z(10)$, $Z(12)$, and $Z(20)$ gauge theory. These cycles were obtained on a 16^3 lattice from the dual spin theory. The smooth curves in the figures are obtained from the leading terms in the high- and low-temperature expansions for planar loops $W_C(\beta)$ for the $Z(N)$ theory. These leading-order results are

$$W_C(\beta) \rightarrow \begin{cases} \exp\{-PNe^{-4\beta}[I_0(4\beta) - I_1(4\beta)]\}, & \beta \rightarrow \infty \\ \exp\left[-A \ln\left(\frac{I_0(\beta)}{I_1(\beta)}\right)\right], & \beta \rightarrow 0 \end{cases} \quad (5.1)$$

where P and A are the loop perimeter and area, respectively. Figures 6(a) and 6(c) are hysteresis cycles of the $U(1)$ theory in three dimensions (12^3 lattice) and five dimensions (4^5 lattice). The solid

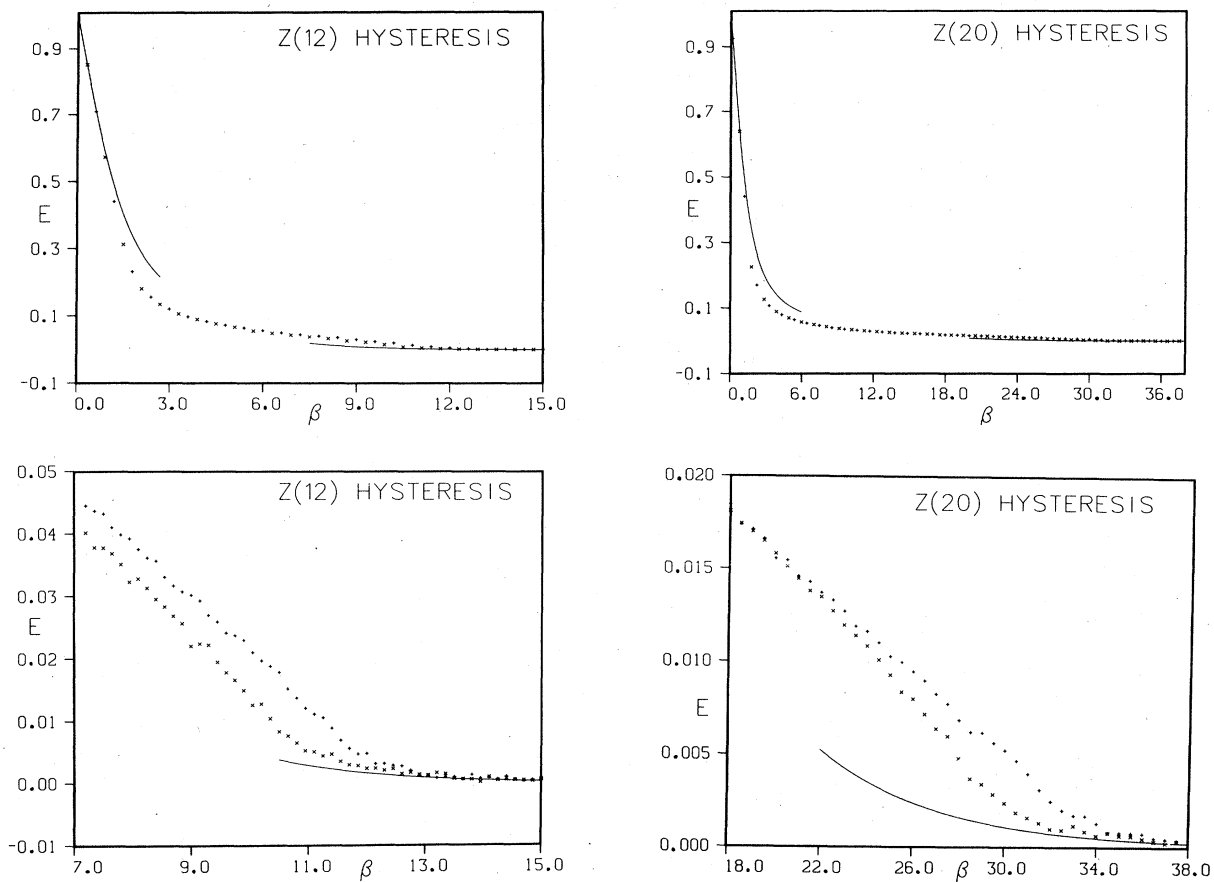
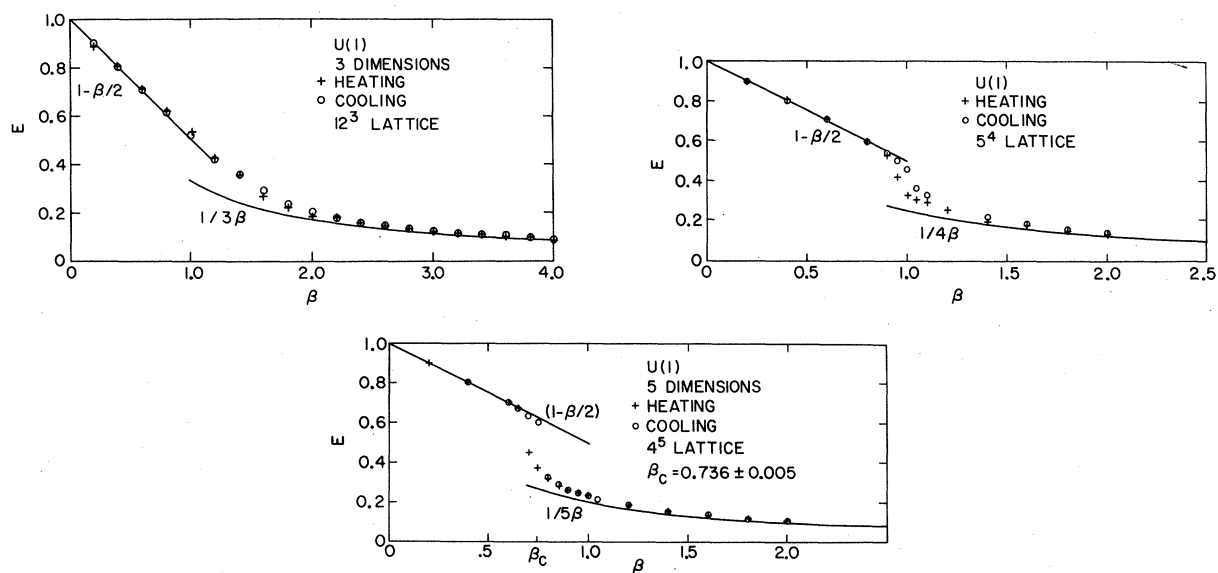


FIG. 5. (Continued).

FIG. 6. Hysteresis cycles in the $U(1)$ gauge theory in three, four, and five dimensions on 12^3 , 5^4 , and 4^5 lattices.

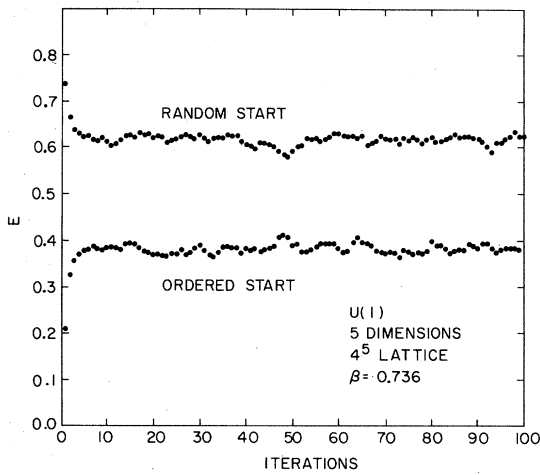


FIG. 7. Iterations from random and ordered lattices at the critical point of the U(1) gauge theory in five dimensions. The figure suggests that the transition is first order.

lines are leading high- and low-temperature expansions. For completeness, we also include the hysteresis cycle of U(1) theory in four dimensions from Ref. 3 [Fig. 6(b)].

The hysteresis effect in five-dimensional U(1) theory is clearly visible. There is also a well-defined hysteresis effect in the $Z(N)$ theories of Fig. 5 which moves out to large β as N increases. The U(1) theory in three dimensions [Fig. 6(a)] seems to be free of a hysteresis effect. This suggests that there is no phase transition in three dimensions in the U(1) theory. Figure 7 is a plot of $E(\beta)$ versus the number of iterations starting from random and ordered configurations for U(1) in five dimensions at the critical point, which we estimate to be at $\beta = 0.736 \pm 0.005$. The two phases remain clearly distinguished after 100 iterations suggesting that the transition is first order. To study the approach of $Z(N)$ to U(1), as $N \rightarrow \infty$, we plot $E(\beta)$ versus β for $Z(2)$, $Z(6)$, $Z(20)$, and U(1) in Fig. 8. In the critical regions, the plotted points are averages of the heating, the cooling cycles. The solid line is the low-temperature U(1) result $E(\beta) \rightarrow 1/3\beta$; $\beta \rightarrow \infty$. Except for $Z(2)$, one expects all these theories to look alike at low β where the high temperatures and consequent near-random assignment of link variables blurs the discreteness of the $Z(N)$ theories. One expects that the $Z(N)$ curves will start deviating substantially from U(1) only when β exceeds the critical point β_{Nc} of the $Z(N)$ theory. For β beyond this point, the $Z(N)$ theory suddenly plunges into an ordered phase. The transition occurs when the temperature is low enough for the discrete nature of the $Z(N)$ field to be apparent. The U(1) theory,

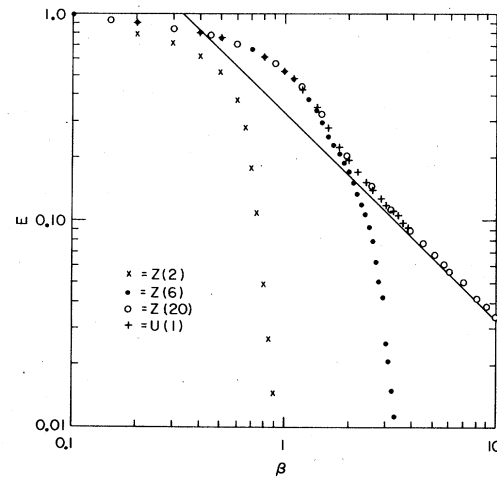


FIG. 8. $E(\beta)$ vs β for $Z(2)$, $Z(6)$, $Z(20)$, and U(1).

on the other hand, remains disordered for arbitrarily large β because of long-wavelength excitations. The data of Fig. 8 support this intuitive picture. There is a significant deviation of $Z(2)$ and $Z(6)$ from U(1) beyond their critical points $\beta_{2c} = 0.7613$ and $\beta_{6c} \sim 2.8$. The $Z(20)$ theory has its critical point at $\beta_{20c} \sim 30$ and shows no deviation from U(1) up to a β of 10.

The hysteresis effects of Fig. 5 are rather weak, particularly for large N . To convince ourselves that they really signal a phase transition and are not artifacts of our calculation procedure, we have studied Wilson loops in the $Z(8)$ theory. Large

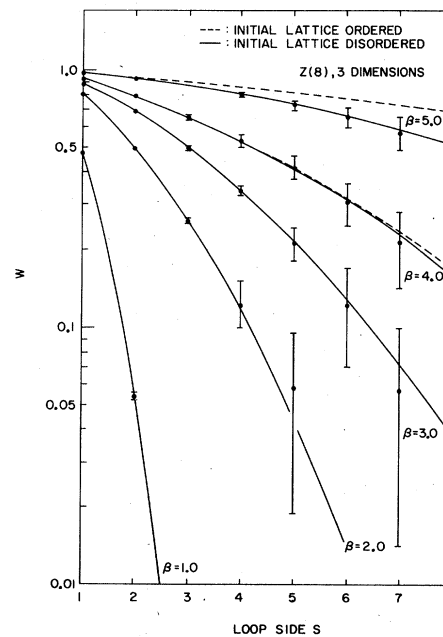


FIG. 9. Square Wilson loops in $Z(8)$ gauge theory. We plot W vs loop side for various values of β .

loops can be used to signal a phase transition. For large loops, $W \sim \exp(-P)$ in the ordered phase and $W \sim \exp(-A)$ in the disordered phase (P and A are the loop perimeter and area, respectively).

In Fig. 9, we present values for square loops W_s versus loop side S for various values of β in $Z(8)$. W_s was calculated at each point as the average over 20 iterations of a 16^3 lattice after 100 iterations at fixed β . The solid and dashed lines are least-square fits to the form

$$W_s(\beta) = \exp[\alpha_1(\beta)S^2 + \alpha_2(\beta)S + \alpha_3(\beta)]. \quad (5.2)$$

We fit to loops of side 1 through 4 and extrapolate to larger S for comparison with data.

Note that the extrapolated curves fit the data points for large S better as β increases. The statistical error is also small once $W \geq 0.2$. For $\beta = 4.0, 5.0$ we plot loops starting both from initially ordered and disordered lattices. One notices in Fig. 9 that for $\beta = 5$, the curves for initially ordered and initially disordered lattices deviate more from one another than for $\beta = 4$. This is what one would expect if there were a critical point near $\beta = 5$. Notice also that this deviation is larger for larger loops. This is because a local action such as the one we use here needs progressively more iterations to bring larger loops to equilibrium.

Figure 10 is a plot of $\alpha_1(\beta)$, the coefficient of the area law, as a function of β . The phase transition in $Z(8)$ is signaled by the vanishing of $\alpha_1(\beta)$

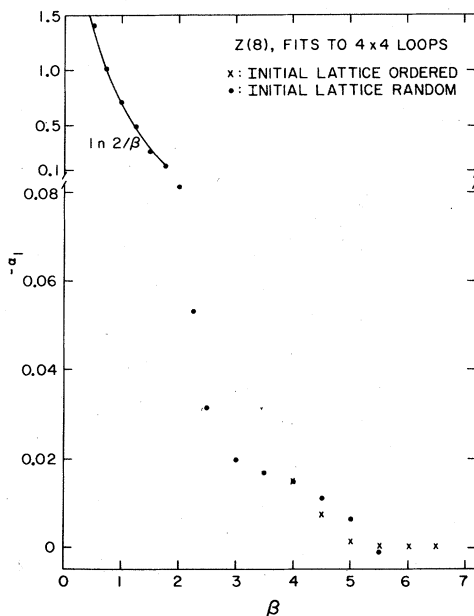


FIG. 10. Coefficient of the area law α_1 in the three-dimensional $Z(8)$ gauge theory as a function of β . Note the zero in this coefficient at $\beta_c \approx 5$.

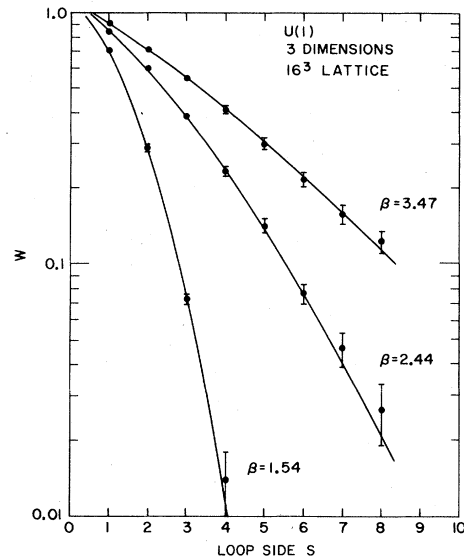


FIG. 11. Square Wilson loops in the $U(1)$ gauge theory.

beyond $\beta \sim 5$. Had the gauge group been continuous instead of discrete, this would have signaled the vanishing of the string tension as a function of the coupling, implying a transition from a confining to an unconfined phase.

We have also studied Wilson loops in the $U(1)$ theory. Figure 11 is a plot of W_s versus S for $U(1)$ on a 16^3 lattice for some representative values of β . Included in this figure are least-square fits to the form in Eq. (5.2). The coefficient of the area law is plotted as a function of β in Fig. 12.

Notice that it does not seem to go to zero over the range of β studied.

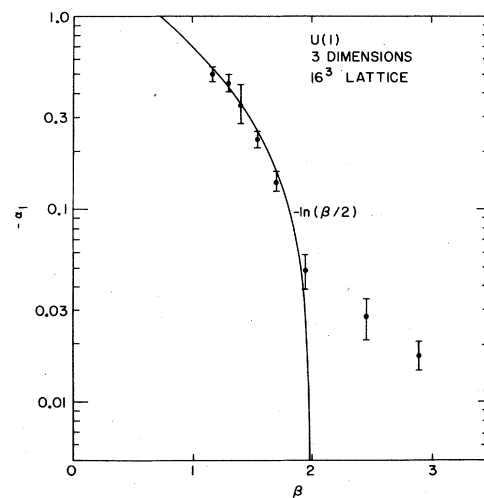


FIG. 12. The string tension α_1 (in units of inverse lattice spacing squared) vs β for $U(1)$ gauge theory in three dimensions. Note the absence of a zero in α_1 over the range of β studied.

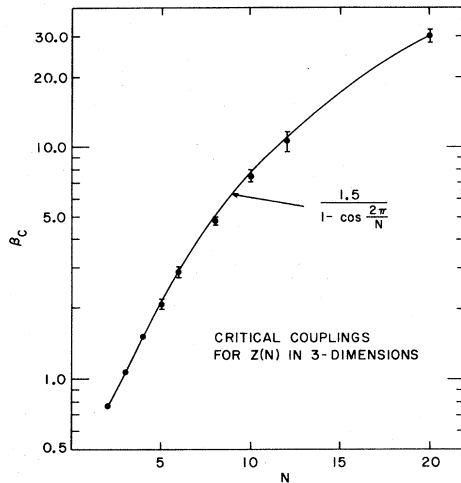


FIG. 13. Critical values β_{Nc} of β for three-dimensional $Z(N)$ theory as a function of N . The figure shows that $\beta_{Nc} \sim (3/4\pi^2)N^2$ for large N .

VI. SUMMARY

We have presented evidence that the $Z(N)$ gauge theory in three dimensions has a single order-

disorder transition at finite temperature. Our estimates of the critical values of β for various N are plotted in Fig. 13 along with known results for $N \leq 4$. The critical point β_{Nc} in $Z(N)$ seems to move off to $\beta = \infty$ roughly as N^2 for large N . This implies that the $U(1)$ theory has only one phase. We have also studied the $U(1)$ theories in three dimensions directly and have found no evidence for a phase transition. Five-dimensional $U(1)$ theory, however, has a critical point at $\beta = 0.736 \pm 0.005$ which seems to be first order.

In closing, we wish to remark that it is encouraging that the zero in the "string tension" at the critical point of $Z(8)$ is seen using fits only to loops of side 4. This may mean that it is not necessary to analyze very large loops to get convincing evidence of a single phase for $SU(3)$ gauge theory.

ACKNOWLEDGMENTS

We wish to thank Barry Freedman and Claudio Rebbi for numerous discussions. This work was supported by the U. S. Department of Energy under Contract No. DE-AC02-76CH00016.

¹K. G. Wilson, Phys. Rev. D **10**, 2445 (1974).

²J. M. Drouffe, G. Parisi, and N. Surlas, Nucl. Phys. **B161**, 397 (1979).

³M. Creutz, L. Jacobs, and C. Rebbi, Phys. Rev. D **20**, 1915 (1979).

⁴L. P. Kadanoff, Rev. Mod. Phys. **49**, 267 (1977).

⁵A. M. Polyakov, Phys. Lett. **59B**, 82 (1975); Nucl. Phys. **B120**, 429 (1977).

⁶S. D. Drell, H. R. Quinn, B. Svetitsky, and M. Weinstein, Phys. Rev. D **19**, 619 (1979).

⁷A physical picture of this transition is given in M. B. Einhorn, E. Rabinovici, and R. Savit, University of Michigan Report No. UM-HE-79-25, 1979 (unpublished).

⁸M. Creutz, Phys. Rev. D **21**, 2308 (1980).

⁹F. Wegner, J. Math. Phys. **12**, 2259 (1971).

¹⁰C. P. Korthals Altes, Nucl. Phys. **B142**, 315 (1978).

¹¹R. Savit, University of Michigan Report No. UM-HE-79-8, 1979 (unpublished).

¹²A. Ukawa, P. Windey, and A. Guth, Phys. Rev. D **21**, 1013 (1980); S. Elitzur, R. B. Pearson, and J. Shigemitsu, *ibid.* **19**, 3698 (1979).

¹³M. Fisher and D. S. Gaunt, Phys. Rev. **133**, A225 (1964).

¹⁴H. W. J. Blöte and R. H. Swendsen, Phys. Rev. Lett. **43**, 799 (1979).

¹⁵M. Suzuki, Prog. Theor. Phys. **37**, 770 (1967).

¹⁶R. Balian, J. M. Drouffe, and C. Itzykson, Phys. Rev. D **11**, 2098 (1975).